Theoretical Insight into the C−C Coupling Reactions of the Vinyl, Phenyl, Ethynyl, and Methyl Complexes of Palladium and Platinum

Valentine P. Ananikov,[†,‡] Djamaladdin G. Musaev,*[,‡] and Keiji Morokuma*[,‡]

N. D. Zelinsky Institute of Organic Chemistry, Russian Academy of Sciences, Leninsky Prospect 47, Moscow 119991, Russia, and Cherry L. Emerson Center for Scientific Computation and Department of Chemistry, Emory University, Atlanta, Georgia 30322

Received November 24, 2004

The mechanism and controlling factors of the C−C reductive elimination reactions of vinyl, phenyl, ethynyl, and methyl ligands from the Pd and Pt complexes $RR'M(PH_3)_2$ were studied with a density functional method. The barrier of C−C coupling from the symmetrical $R_2M(PH_3)_2$ (where M = Pd, Pt) complex decreases in the order R = methyl > ethynyl > phenyl > vinyl, and the exothermicity of the reaction increases in the same order. That is, the methyl−methyl coupling has the highest barrier and smallest exothermicity, while the vinyl−vinyl coupling has the smallest barrier and largest exothermicity. For the asymmetrical $RR'M(PH_3)_2$ complexes, the activation and reaction energies are found to be approximately the average of the corresponding parameters of symmetrical coupling reactions, and this simple rule is expected to be valid for other asymmetrical coupling reactions involving different substituted alkyl, vinyl, phenyl, and ethynyl groups as well as different transition-metal complexes. These C−C coupling reactions occur much more easily in Pd than in Pt complexes, because the Pd−R bonds are weaker than the Pt−R bonds. The major thermodynamic and kinetic factors determining the C−C coupling in these complexes have been discussed. For reactions with similar exothermicities, the kinetics of C−C bond formation is mainly determined by the orientation effect that includes the directionality of the M−C bond and the steric interaction between R and the other ligand (phosphine in the present case), which favors vinyl over phenyl over methyl. However the activation barrier is strongly dominated by exothermicity when it is very different between reactions.

1. Introduction

Transition-metal-catalyzed selective C−C cross-coupling reactions involving the sp^3, sp^2, and sp carbon atoms are well established as a practical tool of synthetic organic and organometallic chemistry.[1−6] Numerous natural products, biologically active compounds, drug precursors, and important organic products were prepared utilizing these methods.[7−12] However, the mechanism and controlling factors of the most important stage, C−C bond formation, still remain unsolved, and their elucidation could lead to discovery of new natural products and drug precursors. Previous experimental studies of the mechanism have been limited to some model studies, while previous theoretical studies of C−C coupling were limited to reactions involving the methyl ligands (Scheme 1, R = R′= CH_3).[13,14] To the best of our knowledge, no detailed theoretical studies on the mechanism and controlling factors of the reductive elimination reactions involving unsaturated carbon ligands (phenyl, vinyl, and ethynyl) have been published, except our recent investigation of vinyl−vinyl coupling reactions.[15,16]

[†] N. D. Zelinsky Institute of Organic Chemistry.
[‡] Emory University.

(1) *Metal-Catalyzed Cross-Coupling Reactions*; Diederich, F., Stang, P. J., Eds.; Wiley-VCH: Weinheim, Germany, 1998.
(2) (a) Suzuki, A.; Brown, H. C. *Organic Synthesis Via Boranes: Suzuki Coupling*; Aldrich Chemical Co.: Milwaukee, WI, 2003; Vol. 3. (b) *Cross-Coupling Reactions: A Practical Guide,* Miyaura, N., Ed.; Springer: Berlin, 2002.
(3) *Handbook of Organopalladium Chemistry for Organic Synthesis*; Negishi, E., Ed.; Wiley: New York and Chichester, U.K., 2002; Vol. 1, pp 215−994.
(4) Tsuji, J. *Palladium Reagents and Catalysts: Innovation in Organic Synthesis*; Wiley & Sons: Chichester, U.K., 1995.
(5) Beletskaya, I. P.; Cheprakov, A. V. Metal Complexes as Catalysts for C−C Cross-Coupling Reactions. In *Comprehensive Coordination Chemistry II*; McCleverty, J. A., Meyer, T. J., Eds.; Elsevier: Oxford, U.K., 2004; Vol. 9, pp 305−368.
(6) (a) Maitlis, P. M. *J. Mol. Catal. A* **2003**, *204−205*, 55. (b) Wang, Z. Q.; Turner, M. L.; Kunicki, A. R.; Maitlis, P. M. *J. Organomet. Chem.* **1995**, *488*, C11.
(7) (a) Suzuki, A. *J. Organomet. Chem.* **1999**, *576,* 147. (b) Miyaura, N.; Suzuki, A. *Chem. Rev.* **1995**, *95,* 2457.
(8) (a) Negishi, E. *Acc. Chem. Res.* **1982**, *15*, 340. (b) Negishi, E. In *Current Trends in Organic Synthesis*; Nozaki, H., Ed.; Pergamon: New York, 1983; pp 269−280.
(9) (a) Beletskaya, I. P. *J. Organomet. Chem.* **1983**, *250*, 551. (b) Bumagin, N. A.; Bumagina, I. G.; Beletskaya, I. P. *Dokl. Akad. Nauk SSSR* **1984**, *274*, 1103. (c) Bumagin, N. A.; Kasatkin A. N.; Beletskaya, I. P. *Izv. Akad. Nauk SSSR, Ser. Khim.* **1983**, 912.
(10) (a) Sonogashira, K. *Compr. Org. Synth.* **1991**, *3*, 521. (b) Sonogashira, K. *Compr. Org. Synth.* **1991**, *3*, 551.
(11) (a) Hiayma, T.; Hatanaka, Y. *Pure Appl. Chem.* **1994**, *66*, 1471. (b) Hayashi, T.; Konishi, M.; Kobori, Y.; Kumada, M.; Higuchi, T.; Hirotsu, K. *J. Am. Chem. Soc.* **1984**, *106,* 158. (c) Siemsen, P.; Livingston, R. C.; Diederich, F. *Angew. Chem., Int. Ed.* **2000**, *39*, 2632.
(12) (a) Stille, J. K. *Angew. Chem., Int. Ed. Engl.* **1986**, *25,* 508. (b) Stille, J. K. *Pure Appl. Chem.* **1985**, *57*, 1771. (c) Mitchell, T. N. *Synthesis* **1992**, 803. (d) Farina, V.; Krishnamurthy, V.; Scott, W. J. The Stille Reaction. In *Organic Reactions*; Wiley: New York, 1997; Vol. 50, p 3.

10.1021/om0490841 CCC: $30.25
Publication on Web 01/22/2005

Scheme 1

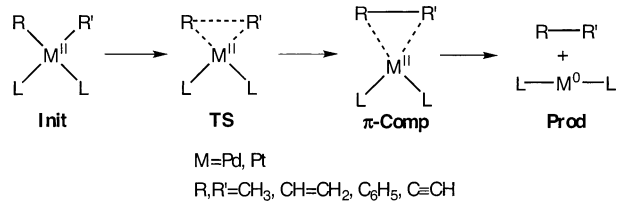

Therefore, in this article we present a comprehensive theoretical study of the mechanisms and controlling factors of the RR′M(PR″$_3$)$_2$-catalyzed (where M = Pd, Pt) reductive elimination reactions of unsaturated ligands (methyl, vinyl, phenyl, and ethynyl) in symmetrical (R = R′) and asymmetrical (R ≠ R′) couplings (Scheme 1). We believe that the findings presented in this article will allow us to gain more insight into the catalytic cross-coupling reaction mechanism and to help to design synthetic procedures involving several competitive routes.

2. Calculation Procedure

Geometries and energetics of the reactants, intermediates, transition states (TSs), and products of the reactions were calculated using the B3LYP hybrid density functional method[17] in conjunction with the standard 6-311G(d) basis set[18] for C, P, and H and the triple-ζ basis set with the Stuttgart/Dresden (relativistic) effective core potentials[19] (SDD) for the metals (Pd and Pt). For all of the stationary points normal-coordinate analysis was performed to characterize the nature of structures, and the thermodynamics was calculated at 298.15 K and 1 atm. For the IRC (intrinsic reaction coordinate) calculations the standard method was used.[20] All calculations were performed without any symmetry constraints using the Gaussian98 program.[21] In our previous studies[15,22] we have established that this level of theory reasonably describes the energy and geometry parameters of the systems involved in the reactions reported in the present paper.

For the symmetrical coupling reaction R$_2$M(PR″$_3$)$_2$ → R−R + M(PR″$_3$)$_2$, the M−R bond dissociation energies (BDE), D(M−R), were calculated using the relationship D(M−R) = (ΔH + D(R−R))/2, where ΔH_r and D(R−R) are the calculated enthalpy of reaction and carbon−carbon single bond dissociation energy, respectively. For the asymmetrical coupling reaction RR′M(PR″$_3$)$_2$ → R−R′ + M(PR″$_3$)$_2$, only the sum of the BDE's of two different metal−carbon bonds can be obtained as D(M−R) + D(M−R′) = ΔH + D(R−R′).

In our calculations we use PH$_3$ as a model for the phosphine ligand (PR″$_3$) (Scheme 1). This approach has been tested in several previous theoretical studies and proven to provide correct relative trends in the reactivity of transition-metal−phosphine complexes.[13−15] For the reductive elimination of the vinyl groups, we studied only the energetically preferred s-trans pathway.[15]

Below we use the notation ***n*_a**, where ***n*** = **1** (R = R′ = CH$_3$), **2** (R = R′= CH=CH$_2$), **3** (R = R′ = C$_6$H$_5$), **4** (R = R′ = C≡CH), **5** (R = CH$_3$ and R′ = CH=CH$_2$), **6** (R = CH$_3$ and R′ = C$_6$H$_5$), **7** (R = CH$_3$ and R′ = C≡CH), **8** (R = CH=CH$_2$ and R′ = C$_6$H$_5$), **9** (R = CH=CH$_2$ and R′ = C≡CH), **10** (R = C≡CH and R′ = C$_6$H$_5$), and stands for the complex, while **a** = **Init**, **TS**, **π-Comp** (or **σ-Comp**), **Prod** and marks the structures (initial reactant, transition state, π (or σ) complex, and product, respectively) on the potential energy surface of the reaction (Scheme 1). In the text, the calculated energetics and geometries corresponding to the Pd complexes will be presented without parentheses, while the corresponding values for Pt compounds will be given in parentheses: i.e., in the manner Pd (Pt). The following abbreviations for organic ligands will be used throughout the article: Me, methyl (CH$_3$); Vin, vinyl (CH=CH$_2$); Ph, phenyl (C$_6$H$_5$); and Eth, ethynyl (C≡CH).

The calculated structural parameters, bond energies, and relative energies (ΔE, ΔH, and ΔG) are summarized in Tables 1−3, respectively. In Table 4, we present the calculated and estimated (see below) energetics for the asymmetrical C−C coupling. The optimized structures are shown in Figures 1 and 2.

3. Results and Discussion

A. Trends in M−C Bond Distances and Bond Energies of the Reactant Complexes. Let us start our discussion from the structure and energetics of the initial complexes **1_Init**−**10_Init**. As seen in Tables 1 and 2, the calculated M−C bond distance and bond dissociation energy (BDE) in these complexes change in the order

M−C bond distance:

$$\text{M−Eth} < \text{M−Vin} < \text{M−Ph} < \text{M−Me}$$

M−C BDE: $\text{M−Eth} > \text{M−Vin} \approx \text{M−Ph} > \text{M−Me}$

for both (Pd and Pt) metals. These trends are in excellent agreement with available experimental data[23] and could be attributed to the increase of s character in the hybridized carbon orbital (sp > sp^2 > sp^3). The trend in BDE also correlates with that in the calculated BDE of the central C−C bond of organic products: diacetylene > butadiene ≈ biphenyl > ethane (see Table S1 in the Supporting Information).

In general, in all cases the Pt−C bonds are found to be about 8 kcal/mol stronger than the corresponding Pd−C bonds (Table 2), which is in excellent agreement with our previous explanations.[15]

(13) For representative studies see: (a) Tatsumi, K.; Hoffmann, R.; Yamamoto, A.; Stille, J. K. *Bull. Chem. Soc. Jpn.* **1981**, *54*, 1857. (b) Low, J. L.; Goddard, W. A. *J. Am. Chem. Soc.* **1986**, *108*, 6115. (c) Low, J. L.; Goddard, W. A. *Organometallics* **1986**, *5*, 609. (d) Koga, N.; Morokuma, K. *Organometallics* **1991**, *10*, 946. (e) Blomberg, M. R. A., Siegbahn, P. E. M.; Nagashina, U.; Wennerberg, J. *J. Am. Chem. Soc.* **1991**, *113*, 424. (f) Siegbahn, P. E. M.; Blomberg, M. R. A. *J. Am. Chem. Soc.* **1992**, *114,* 10548. (g) Sakaki, S.; Ieki, M. *J. Am. Chem. Soc.* **1993**, *115,* 2373. (h) Sakaki, S.; Ogawa, M.; Musashi, Y.; Arai, T. *Inorg. Chem.* **1994**, *33*, 1660. (i) Sakaki, S.; Mizoe, N.; Musashi, Y.; Biswas, B.; Sugimoto, M. *J. Phys. Chem. A* **1998**, *102,* 8027. (j) Hill, G. S.; Puddephatt, R. J. *Organometallics* **1998**, *17*, 1478. (k) Cao, Z.; Hall, M. B. *Organometallics* **2000**, *19*, 3338. (l) Sundermann, A.; Uzan, O.; Milstein, D.; Martin, J. M. L. *J. Am. Chem. Soc.* **2000**, *122*, 7095. (m) Sundermann, A.; Uzan, O.; Martin, J. M. L. *Organometallics* **2001**, *20*, 1783.

(14) For general reviews see: (a) Didieu, A. *Chem. Rev.* **2000**, *100*, 543. (b) Musaev, D. G.; Morokuma, K. *Top. Catal.* **1999**, *7*, 107. (c) Siegbahn, P. E. M.; Blomberg, M. R. A. In *Theoretical Aspects of Homogeneous Catalysis, Applications of Ab Initio Molecular Orbital Theory*; van Leeuwen, P. W. N. M., van Lenthe, J. H., Morokuma, K., Eds.; Kluwer Academic: Dordrecht, The Netherlands, 1995. (d) Koga, N.; Morokuma, K. *Chem. Rev.* **1991**, *91,* 823.

(15) Ananikov, V. P., Musaev D. G., Morokuma, K. *J. Am. Chem. Soc.* **2002**, *124*, 2839.

(16) For a coupling of two sp^2 carbon atoms in metallabenzenes, see: Iron, M. A.; Martin, J. M. L.; van der Boom, M. E. *J. Am. Chem. Soc.* **2003**, *125*, 13020.

(17) (a) Becke, A. D. *Phys. Rev. A* **1988**, *38*, 3098. (b) Lee, C.; Yang, W.; Parr, R. G. *Phys. Rev. B* **1988**, *37*, 785. (c) Becke, A. D. *J. Chem. Phys.* **1993**, *98*, 5648.

(18) (a) Krishnan, R.; Binkley, J. S.; Seeger, R.; Pople, J. A. *J. Chem. Phys.* **1980**, *72*, 650. (b) McLean, A. D.; Chandler, G. S. *J. Chem. Phys.* **1980**, *72*, 5639.

(19) (a) Schwerdtfeger, P.; Dolg, M.; Schwarz, W. H.; Bowmaker, G. A.; Boyd, P. D. W. *J. Chem. Phys.* **1989**, *91*, 1762. (b) Andrae, D.; Haubermann, U.; Dolg, M.; Stoll, H.; Preuss, H. *Theor. Chim. Acta* **1990**, *77*, 123. (c) Bergner, A.; Dolg, M.; Küchle, W.; Stoll, H.; Preuss, H. *Mol. Phys.* **1993**, *80*, 1431.

(20) (a) Gonzalez, C.; Schlegel, H. B. *J. Chem. Phys.* **1989**, *90*, 2154. (b) Gonzalez, C.; Schlegel, H. B. *J. Phys. Chem.* **1990**, *94*, 5523.

Table 1. Calculated Selected Bond Lengths (in Å) and Angles (in deg) for the Studied Complexes $RR'M(PH_3)_2$[a,b]

no.	R	R′	structure	M−C[c]	M−C′[c]	M−P[d]	M−P′[d]	C−C′[c]	C−M−C′[c]	P−M−P′[d]	tilt angle[e]
1	CH_3	CH_3	**Init**	2.100	2.100	2.367	2.367	2.778	82.8	102.3	0.8
				(2.108)	(2.108)	(2.340)	(2.340)	(2.811)	(83.6)	(100.8)	(0.9)
			TS	2.198	2.198	2.384	2.384	2.071	56.2	111.4	52.0
				(2.270)	(2.270)	(2.312)	(2.312)	(2.022)	(52.9)	(118.9)	(59.5)
2	$CH{=}CH_2$	$CH{=}CH_2$	**Init**	2.052	2.052	2.376	2.376	2.716	82.9	105.1	1.5
				(2.062)	(2.062)	(2.354)	(2.354)	(2.777)	(84.7)	(102.1)	(0.3)
			TS	2.070	2.070	2.391	2.391	2.021	58.4	106.8	0.3
				(2.103)	(2.103)	(2.346)	(2.346)	(1.845)	(52.0)	(104.2)	(6.1)
3	Ph	Ph	**Init**	2.065	2.065	2.383	2.383	2.781	84.6	103.9	0.0
				(2.077)	(2.077)	(2.357)	(2.357)	(2.853)	(86.8)	(101.4)	(1.2)
			TS	2.109	2.109	2.407	2.407	1.998	56.5	106.1	1.7
				(2.160)	(2.160)	(2.352)	(2.352)	(1.843)	(50.5)	(106.9)	(2.9)
4	C≡CH	C≡CH	**Init**	1.988	1.988	2.352	2.352	2.809	89.9	105.3	0.0
				(1.999)	(1.999)	(2.340)	(2.340)	(2.841)	(90.6)	(102.6)	(0.0)
			TS	1.994	1.994	2.395	2.395	1.848	55.2	107.5	0.1
				(2.049)	(2.049)	(2.351)	(2.351)	(1.648)	(47.4)	(107.3)	(0.0)
5	CH_3	$CH{=}CH_2$	**Init**	2.096	2.046	2.383	2.380	2.774	84.1	101.7	0.5
				(2.106)	(2.055)	(2.355)	(2.353)	(2.820)	(85.3)	(100.3)	(0.5)
			TS	2.219	2.059	2.387	2.404	2.000	55.6	105.2	18.0
				(2.289)	(2.090)	(2.320)	(2.347)	(1.912)	(51.5)	(107.8)	(28.3)
6	CH_3	Ph	**Init**	2.103	2.065	2.382	2.365	2.770	83.3	102.9	0.0
				(2.110)	(2.076)	(2.354)	(2.342)	(2.818)	(84.6)	(101.1)	(0.0)
			TS	2.242	2.093	2.399	2.405	1.989	54.5	104.6	8.9
				(2.324)	(2.133)	(2.321)	(2.345)	(1.919)	(50.8)	(108.4)	(27.0)
7	CH_3	C≡CH	**Init**	2.093	1.998	2.401	2.337	2.805	86.5	103.5	0.9
				(2.109)	(2.002)	(2.373)	(2.315)	(2.828)	(86.9)	(101.6)	(0.5)
			TS	2.277	1.988	2.399	2.409	1.897	52.3	105.9	18.0
				(2.378)	(2.021)	(2.328)	(2.349)	(1.822)	(48.1)	(109.3)	(21.5)
8	$CH{=}CH_2$	Ph	**Init**	2.051	2.067	2.384	2.373	2.741	83.5	104.2	0.8
				(2.059)	(2.079)	(2.360)	(2.349)	(2.803)	(85.3)	(101.6)	(0.6)
			TS	2.080	2.101	2.404	2.394	1.997	57.1	106.3	1.1
				(2.118)	(2.145)	(2.354)	(2.344)	(1.839)	(51.1)	(105.0)	(7.1)
9	$CH{=}CH_2$	C≡CH	**Init**	2.042	2.002	2.399	2.338	2.758	86.0	104.9	0.7
				(2.058)	(2.006)	(2.378)	(2.320)	(2.801)	(87.1)	(102.1)	(0.8)
			TS	2.090	1.997	2.401	2.392	1.912	55.7	107.4	2.0
				(2.090)	(2.029)	(2.347)	(2.351)	(1.737)	(49.0)	(105.8)	(7.7)
10	Ph	C≡CH	**Init**	2.057	1.998	2.397	2.347	2.781	86.6	104.5	0.1
				(2.076)	(2.002)	(2.375)	(2.327)	(2.834)	(88.0)	(102.2)	(0.1)
			TS	2.110	1.998	2.400	2.403	1.915	55.5	106.8	0.3
				(2.182)	(2.035)	(2.342)	(2.358)	(1.733)	(48.4)	(106.6)	(0.2)

[a] Values for M = Pd are given without parentheses, while those for M = Pt are given in parentheses. [b] The imaginary frequencies (in cm^{-1} for **1-TS**−**10-TS**, respectively) are: 481 (530) *i*, 378 (450) *i*, 323 (357) *i*, 428 (336) *i*, 467 (531) *i*, 425 (481) *i*, 472 (505) *i*, 363 (415) *i*, 406 (398) *i*, 366 (337) *i*. [c] C and C′ atoms belong to R and R′, respectively. [d] P is trans to R, and P′ is trans to R′. [e] The absolute value of the angle between P−M−P′ and C−M−C′ planes.

Table 2. Sum of M−R and M−R′ Bond Dissociation Energies, BDE(M−R) + BDE(M−R′) (in kcal/mol) and the Predicted Values for Asymmetric Complexes from the Value from Symmetric Complexes[a]

		M = Pd		M = Pt	
no.	complex	calcd	predicted[a]	calcd	predicted[a]
1	$M(CH_3)_2(PH_3)_2$	28.5 × 2		36.0 × 2	
2	$M(CH{=}CH_2)_2(PH_3)_2$	38.6 × 2		46.4 × 2	
3	$M(Ph)_2(PH_3)_2$	38.8 × 2		46.5 × 2	
4	$M(C{\equiv}CH)_2(PH_3)_2$	73.5 × 2		82.1 × 2	
5	$M(CH_3)(CH{=}CH_2)(PH_3)_2$	67.5	67.1	82.4	82.4
6	$M(CH_3)(Ph)(PH_3)_2$	67.5	67.3	82.9	82.5
7	$M(CH_3)(C{\equiv}CH)(PH_3)_2$	104.6	102.0	116.6	118.1
8	$M(CH{=}CH_2)(Ph)(PH_3)_2$	77.4	77.4	93.1	92.9
9	$M(CH{=}CH_2)(C{\equiv}CH)(PH_3)_2$	113.4	112.1	129.5	128.5
10	$M(Ph)(C{\equiv}CH)(PH_3)_2$	113.7	112.3	129.7	128.6

[a] See text for more details.

Strikingly, the sum of the M−R and M−R′ BDEs for the asymmetrical complexes **5_Init**−**10_Init** is very close to the sum of the corresponding values calculated independently for the symmetrical complexes **1_Init**−**4_Init** (see Table 2). This suggests that the M−C BDE

(21) Frisch, M. J.; Trucks, G. W.; Schlegel, H. B.; Scuseria, G. E.; Robb, M. A.; Cheeseman, J. R.; Zakrzewski, V. G.; Montgomery, J. A., Jr.; Stratmann, R. E.; Burant, J. C.; Dapprich, S.; Millam, J. M.; Daniels, A. D.; Kudin, K. N.; Strain, M. C.; Farkas, O.; Tomasi, J.; Barone, V.; Cossi, M.; Cammi, R.; Mennucci, B.; Pomelli, C.; Adamo, C.; Clifford, S.; Ochterski, J.; Petersson, G. A.; Ayala, P. Y.; Cui, Q.; Morokuma, K.; Malick, D. K.; Rabuck, A. D.; Raghavachari, K.; Foresman, J. B.; Cioslowski, J.; Ortiz, J. V.; Stefanov, B. B.; Liu, G.; Liashenko, A.; Piskorz, P.; Komaromi, I.; Gomperts, R.; Martin, R. L.; Fox, D. J.; Keith, T.; Al-Laham, M. A.; Peng, C. Y.; Nanayakkara, A.; Gonzalez, C.; Challacombe, M.; Gill, P. M. W.; Johnson, B. G.; Chen, W.; Wong, M. W.; Andres, J. L.; Head-Gordon, M.; Replogle, E. S.; Pople, J. A. *Gaussian 98*; Gaussian, Inc.: Pittsburgh, PA, 1998.

(22) Ananikov, V. P.; Musaev, D. G.; Morokuma, K. *Organometallics* **2001**, *20*, 1652.

(23) (a) Anderson, G. K. Platinum−Carbon σ-Bonded Complexes. In *Comprehensive Organometallic Chemistry II*; Abel, E. W., Stone, F. G. A., Wilkinson, G., Eds.; Elsevier: Oxford, U.K., 1995; Vol. 9, pp 431−531. (b) Canty, A. J. Palladium−Carbon σ-Bonded Complexes. In *Comprehensive Organometallic Chemistry II*. Abel, E. W., Stone, F. G. A., Wilkinson, G., Eds.; Elsevier: Oxford, U.K., 1995; Vol. 9, pp 225−290.

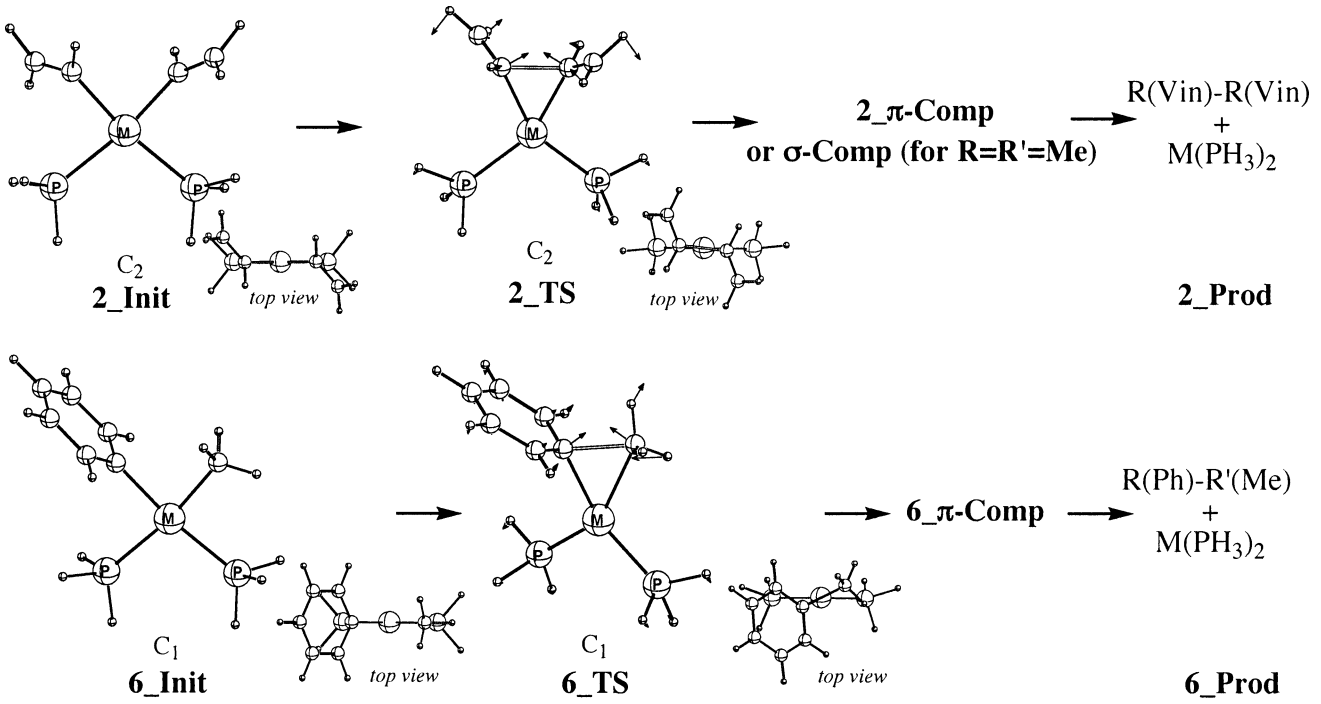

Figure 1. Schematic presentation of the symmetrical (for the case of R = R′ = Vin) and unsymmetrical (for the case of R = Ph and R′ = Me) R−R′ coupling reactions of the complexes RR′M(PH$_3$)$_2$. Optimized structures of initial complexes and transition states for all studied complexes are presented in Figures S1 and S2 in the Supporting Information. Their important geometries are presented in Table 1. Structures of the π and σ complexes are given in Figure 2, while those of the products are presented in Figure S4 (Supporting Information).

is not influenced in a significant manner by interaction between the organic ligands.

Calculated M−C bond distances are in good agreement with their X-ray-determined values. For the asymmetrical alkenyl(alkynyl)Pt complex Pt−C$_{alkenyl}$ = 2.05(2) Å and Pt−C$_{alkynyl}$ = 1.97(2) Å were found experimentally,[24] compared to 2.058 and 2.006 Å for **9_Init** (Table 1). For the phenyl(alkynyl)Pt complex Pt−C$_{phenyl}$ = 2.056(9) Å and Pt−C$_{alkynyl}$ = 1.999(11) Å were experimentally reported,[25] compared to 2.076 and 2.002 Å for **10_Init** (Table 1). Similarly, the calculated M−C bond lengths reproduce experimentally observed trends for dimethyl,[26] dialkynyl,[27] and methyl vinyl[28] complexes.

After discussing the initial complexes, it is natural to elucidate the reaction mechanisms of C−C coupling in these species. Here, we will divide our discussion into four parts. First, we will discuss the reductive elimination reactions from the symmetrical complexes R$_2$M(PH$_3$)$_2$. In the second part, we will discuss the same reactions for the asymmetrical complexes RR′M(PH$_3$)$_2$ and compare the calculated trends with those for the symmetrical species R$_2$M(PH$_3$)$_2$. In the third section we will elucidate the role of the transition-metal center by comparing the data for Pd and Pt complexes, and in the final section we will compare our results with the available experimental data.

B. Reductive Elimination from the Symmetrical R$_2$M(PH$_3$)$_2$ Complexes (M = Pd, Pt). As expected, reductive elimination proceeds through the three-centered transition state (TS) (Figure 1; see also Figure S1 in the Supporting Information), which was confirmed by the IRC calculations to be the real TS for the C−C coupling reaction connecting the reactant and the product complex.

As seen in Table 1, the TS for the Me−Me coupling has a nonplanar structure with a tilt angle of >50°, while for the other symmetric coupling processes studied here it is almost planar with a tilt angle of <7°. Interestingly, for the asymmetrical coupling processes, the largest tilt angle, 9−18° for Pd (22−28° for Pt), corresponds to the Me−R coupling (R = Vin, Ph, Eth). In other words, the process involving Me ligands always proceeds via a nonplanar transition state, and the degree of the nonplanarity is correlated with the number of Me ligands involved. We believe that the observed difference in the tilt angle in these TS structures for different R is the result of (a) a weaker M−C bond (the M−Me BDE is smaller than that for other M−R bonds studied here; see Table 2), (b) the directionality of the M−C bond, which is more profound for M−Me than for other M−R bonds, and (c) steric factors. To support this statement, we performed a series of constrained-geometry optimizations[29] for the vinyl complex Pt(CH=CH$_2$)$_2$(PH$_3$)$_2$ and found that when a larger M−C distance (2.35 Å) is assumed, the M−Vin interaction is very

(24) Stang, P. J.; Kowalski, M. H. *J. Am. Chem. Soc.* **1989**, *111*, 3356.
(25) Muller, C.; Iverson, C. N.; Lachicotte, R.; Jones, W. D. *J. Am. Chem. Soc.* **2001**, *123*, 9718.
(26) (a) Wisner, J. M.; Bartczak, T. J.; Ibres, J. A. *Organometallics* **1986**, *5*, 2044. (b) Wisner, J. M.; Bartczak, T. J.; Ibres, J. A.; Low, J. J.; Goddard, W. A. *J. Am. Chem. Soc.* **1986**, *108*, 347. (c) Haar, C. M.; Nolan, S. P.; Marshall, W. J.; Moloy, K. G.; Prock, A.; Giering, W. P. *Organometallics* **1999**, *18*, 474. (d) Smith, D. C.; Haar, C. M.; Stevens, E. D.; Nolan, S. P. *Organometallics* **2000**, *19*, 1427. (e) de Graaf, W.; Boersma, J.; Smeets, W. J. J.; Spek, A. L.; van Koten, G. *Organometallics* **1989**, 8, 2907.
(27) (a) Phillips, J. R.; Miller, G. A.; Trogler, W. C. *Acta Crystallogr., Sect. C* **1990**, C90, 1648. (b) Falvello, L. R.; Fornies, J.; Gomez, J.; Lalinde, E.; Martin, A.; Moreno, M. T.; Sacristan, J. *Chem. Eur. J.* **1999**, *5*, 474.
(28) Ozawa, F.; Hikida, T. *Organometallics* **1996**, *15*, 4501.

Table 3. Calculated Activation Energy ($\Delta E^{\ddagger}$, $\Delta H^{\ddagger}$, $\Delta G^{\ddagger}$)[a] and Energy of Reaction (ΔE, ΔH, ΔG)[b] for $RR'M(PH_3)_2 \rightarrow R\text{-}R' + M(PH_3)_2$ (in kcal/mol, at 298.15 K and 1 atm)[c]

no.	complex	$\Delta E^{\ddagger}$	ΔE	$\Delta H^{\ddagger}$	ΔH	$\Delta G^{\ddagger}$	ΔG
1	$M(CH_3)_2(PH_3)_2$	25.2 (45.9)	−31.4/−31.5 (−16.2/−16.3)	24.2 (44.8)	−30.4/−31.3 (−15.4/−15.5)	23.6 (45.0)	−41.7/−35.7 (−26.3/−19.9)
2	$M(CH{=}CH_2)_2(PH_3)_2$	6.8 (19.3)	−33.8/−42.5 (−17.8/−27.7)	5.9 (18.1)	−33.2/−41.2 (−17.5/−26.7)	6.0 (18.4)	−44.5/−42.2 (−29.0/−27.2)
3	$M(Ph)_2(PH_3)_2$	11.7 (28.1)	−31.4/−28.2 (−15.7/−7.5)	10.5 (26.5)	−31.1/−27.9 (−15.6/−7.1)	10.7 (26.2)	−41.9/−29.0 (−26.8/−8.2)
4	$M(C{\equiv}CH)_2(PH_3)_2$	14.6 (29.6)	−17.5/−28.8 (−0.3/−15.3)	13.0 (27.6)	−18.1/−28.8 (−0.8/−15.7)	11.3 (25.8)	−29.1/−30.5 (−11.6/−16.0)
5	$M(CH_3)(CH{=}CH_2)(PH_3)_2$	15.9 (33.4)	−30.6/−38.4 (−15.0/−24.6)	15.5 (32.2)	−29.4/−36.3 (−14.5/−23.3)	14.1 (33.5)	−42.0/−37.7 (−25.0/−22.2)
6	$M^{II}(CH_3)(Ph)(PH_3)_2$	18.7 (37.8)	−30.4/−27.2 (−14.9/−6.7)	17.5 (36.4)	−30.0/−26.7 (−14.6/−6.2)	16.9 (37.5)	−41.9/−27.6 (−25.9/−6.1)
7	$M^{II}(CH_3)(C{\equiv}CH)(PH_3)_2$	21.3 (39.8)	−21.3/−29.9 (−5.6/−18.3)	20.6 (38.3)	−20.7/−29.1 (−5.7/−17.5)	18.5 (38.1)	−33.0/−29.0 (−16.5/−16.5)
8	$M^{II}(CH{=}CH_2)(Ph)(PH_3)_2$	9.8 (24.5)	−31.7/−40.7 (−15.9/−26.3)	8.6 (23.1)	−31.4/−39.6 (−15.7/−25.3)	8.7 (22.8)	−43.5/−40.3 (−27.6/−25.0)
9	$M^{II}(CH{=}CH_2)(C{\equiv}CH)(PH_3)_2$	11.5 (25.9)	−22.6/−32.9 (−6.5/−19.5)	10.2 (24.3)	−22.8/−32.3 (−6.7/−18.8)	9.5 (23.4)	−34.7/−33.3 (−18.6/−19.1)
10	$M^{II}(Ph)(C{\equiv}CH)(PH_3)_2$	12.2 (27.2)	−23.2/−32.3 (−7.2/−20.9)	10.8 (25.4)	−23.6/−32.9 (−7.6/−20.3)	10.4 (24.5)	−35.1/−29.7 (−18.9/−19.9)

[a] $\Delta E^{\ddagger}/\Delta H^{\ddagger}/\Delta G^{\ddagger} = E/H/G(\mathbf{TS}) - E/H/G(\mathbf{Init})$. [b] $\Delta E/\Delta H/\Delta G = E/H/G(\mathbf{Prod}) - E/H/G(\mathbf{Init})$. The values after the slant correspond to $E/H/G(\mathbf{Comp}) - E/H/G(\mathbf{Init})$. [c] Values for M = Pd are given without parentheses, while those for M = Pt are given in parentheses.

weak, and the structure becomes nonplanar with a large tilt angle of 59.3° (see Table S2 and Figure S3 in the Supporting Information). One should note that in the transition state **1_TS** of the methyl complex $[Pt(CH_3)_2(PH_3)_2]$ a tilt angle of 59.5° was found with a Pt−C distance of 2.27 Å (Table 1), which is close to the above value for $Pt(CH{=}CH_2)_2(PH_3)_2$ at 2.35 Å.

The difference in M−C bond distances between the transition state and the reactant (Δ(M−C)) shows that the reductive elimination in $(Me)_2M(PH_3)_2$ proceeds through a later transition state than the other reactions studied (Table 1). For the methyl ligand the Δ(M−C) value is 0.098 Å (0.162 Å), while for Ph, Vin, and Eth the Δ(M−C) values are in the range of 0.006−0.044 Å (0.041−0.083 Å).

In agreement with geometry trends, reductive elimination of ethane (R = Me) requires a higher C−C coupling barrier than other ligands (Table 3). That is, the calculated barrier decreases in the order

$$(Me)_2M(PH_3)_2 > (Eth)_2M(PH_3)_2 > (Ph)_2M(PH_3)_2 > (Vin)_2M(PH_3)_2$$

Thus, reductive elimination of two vinyl groups leading to buta-1,3-diene requires a lower coupling barrier, $\Delta H^{\ddagger}$ = 5.9 (18.1) kcal/mol, while reductive elimination of two methyl groups leading to ethane requires a much higher barrier, $\Delta H^{\ddagger}$ = 24.2 (44.8) kcal/mol.

All reductive elimination reactions studied here are exothermic. For both metals the exothermicity of the reaction decreases in the order

$$Vin{-}Vin \approx Ph{-}Ph \approx Me{-}Me > Eth{-}Eth$$

Thus, the butadiyne formation is less exothermic by about 14 kcal/mol than the other symmetric C−C coupling reactions.

Overcoming the transition states leads to the weakly bound complexes. In the case of the Me−Me coupling reaction, the result is the weakly (<1 kcal/mol) bound σ-complex **1_σ-Comp** (see Table 3 and Figure 2). However, in the case of unsaturated ligands, the corresponding π complexes are formed (**2_π-Comp**−**10_π-Comp**, Figure 2). The stability of these π complexes relative to the dissociated products **Prod,** $M(PH_3)_2$ + R−R′, decreases in the order Eth > Vin > Ph (Table 3). For the Eth and Vin ligands the complexation energy is 8−9 (10−12) and 9−11 (13−15) kcal/mol, respectively (Table 3). In contrast, for the Ph ligand the formation of the **3_π-Comp** and **6_π-Comp** complexes from the corresponding **Prod** species is endothermic and proceeds through a transition state.[30] The Pt−C distance in π complexes is shorter than the corresponding Pd−C distance (Figure 2), in agreement with the above energy trend.

At the next stage these weakly bound complexes release the final C−C coupling products (see Figure S4 in the Supporting Information). According to the calculations the entire coupling reactions involving ethynyl groups are less exothermic, suggesting the possible reversibility of the process. Indeed, the reverse process, $C(sp^2){-}C(sp)$ bond activation, has been reported for a Pt(0) complex in the literature.[25] It was shown that under photolysis conditions oxidative addition of the aryl−alkynyl bond occurs to form an asymmetrical aryl(alkynyl)platinum(II) complex (an analogue of **10_Init**). The product complex undergoes reductive elimination upon heating in solution, and the experimental study has indicated this reaction to be downhill thermody-

(29) With the transition state geometry **2_TS** as the starting point, a series of constrained optimizations were performed, keeping the C−C bond distance at 1.845 Å and varying the Pt−C bond lengths in the range 2.103−3.000 Å (Table S2). All the other geometry parameters were optimized.

(30) Three different binding positions are available for the phenyl ring; the calculations have suggested a 2,3-η^2 complex as being more energetically favored. See examples of different complexes and dissociation transition states in Figure S6.

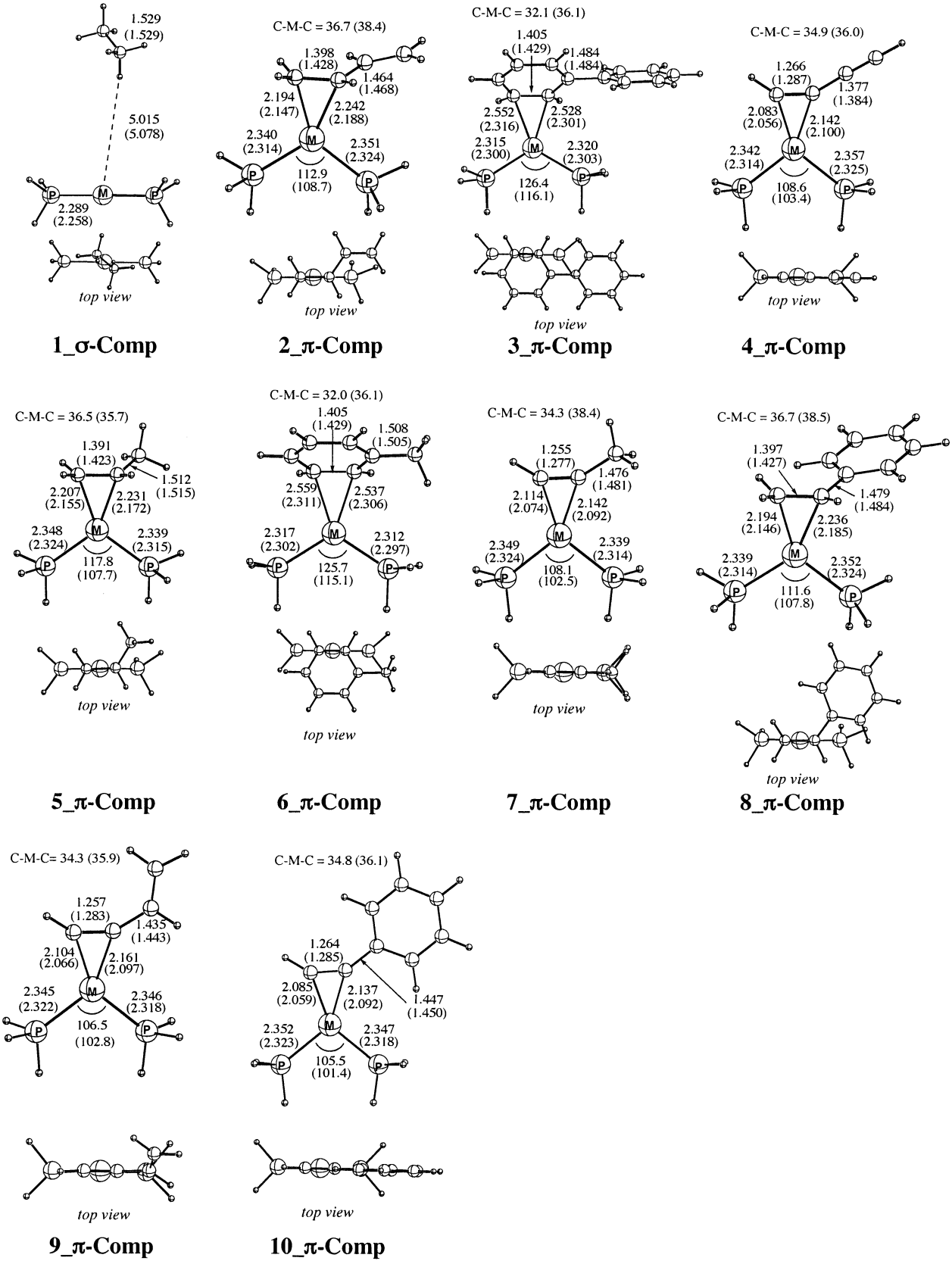

Figure 2. Optimized important geometry parameters of the intermediate complexes (distances in Å and angles in deg) of the C−C coupling reaction from the RR′M(PH_3)$_2$ complexes. Values for M = Pd are given without parentheses, while those for M = Pt are given in parentheses.

namically.[25] These qualitative observations are consistent with the calculated energetics (Table 3).

Note that the inclusion of entropy corrections (Gibbs free energies) only slightly (1−3 kcal/mol) reduces the calculated barriers while it significantly (by 10−12 kcal/mol) increases the exothermicity of the reactions. However, it does not alter the conclusions based on the calculated enthalpies.

Scheme 2

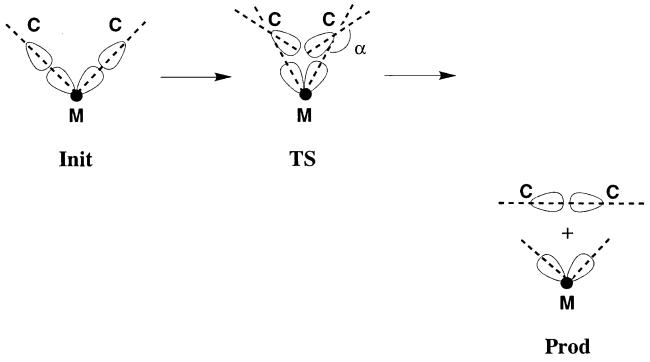

Thermodynamic and Kinetic Factors Controlling the Reductive Elimination Reaction. Above we have shown that the barrier of C−C coupling in the symmetric $R_2M(PH_3)_2$ complexes of Pd and Pt decreases in the order Me−Me > Eth−Eth > Ph−Ph > Vin−Vin, while the exothermicity of the reaction changes in the order Vin−Vin ≈ Ph−Ph ≈ Me−Me > Eth−Eth. These trends could be rationalized by analyzing (1) the M−R and R−R bonding energies and (2) the nature of the R ligand, M−R bond, and the transition state.

The calculated M−R and R−R BDE's decrease in the order M−Eth (for instance, 73.5 kcal/mol for Pd) > M−Vin (38.8) ≈ M−Ph (38.6) > M−Me (28.5) (Table 2) and Eth−Eth (165.1) > Vin−Vin (110.4) ≈ Ph−Ph (108.7) > Me−Me (87.4) (Table S1), respectively. As discussed above, the exothermicity of the coupling reaction is equal to the R−R BDE minus twice the M−R BDE. The fact that the exothermicity for Eth−Eth coupling is the smallest could be explained by the fact that (although the Eth−Eth bond is the strongest R−R bond and the M−Eth bond is the strongest M−R bond) the strength of the formed Eth−Eth bond (over other R−R bonds) is not as large as the strength of the two broken M−Eth bonds (over other M−R bonds).

However, this explanation cannot be used for the C−C bond formation barriers. For this purpose, a detailed analysis of the nature of the M−R bond as well as the character of structural and electronic perturbations to the initial complex induced by the C−C coupling transition state is necessary. Indeed, the C−C bond formation process in these complexes requires reorganization of the bonding M−C orbitals by gradually changing the orientation of the C hybrid (sp^n) orbitals from M centers toward each other (C atoms; see Scheme 2). Therefore, one may expect the R ligand with a more strongly directional C hybrid (sp^n) orbital to have a later transition state and a higher C−C coupling barrier. To test this idea, we performed calculations on the model complexes $RM^{II}(PH_3)_3^+$, where R = Me, Vin, Ph, Eth, and M = Pd, Pt. $RM^{II}(PH_3)_3^+$ contains only one R ligand, to avoid possible steric interaction between the R ligands. A series of constrained-geometry optimization[31] calculations were performed to determine the dependence of the energy on the orientation of R. In these calculations, we chose the angle α (see Scheme 2 and Figure S4 for the definition of α) to be the reaction coordinate and varied it from 180 to 130° with a 10° step, covering the region from the initial complex (α = 180°) to the transition state (α ≈ 145−160°).[32]

It was found that the methyl with an sp^3 hybrid orbital is most sensitive to the orientation change (Tables S3 and S4). The energy of $MeM^{II}(PH_3)_3^+$ increases by 25.5 (31.1) kcal/mol upon decreasing the α angle from 180 to 130°. $VinM^{II}(PH_3)_3^+$ with an sp^2 hybrid vinyl ligand is less sensitive to the same orientation change; the energy increases by 10.0 (10.9) kcal/mol upon decreasing the α angle from 180 to 130°. In general, the sensitivity to the orientation change in this model system decreases in the order R = Me [25.5 (31.1)] > Ph [16.4 (19.4)] > Eth [13.5 (15.1)] > Vin [10.0 (10.9)]. The difference among the complexes $RM^{II}(PH_3)_3^+$ with R = Eth, Ph, Vin ligands having an sp (Eth) or sp^2 hybrid orbital could be explained by steric repulsion between R and PH_3 ligands. One should note that a change in the orientation of the M−C bond affects other geometrical parameters of the system. Indeed, upon decreasing α (a) the M−C bond becomes longer and weaker, (b) the M−P bond becomes shorter due to the weaker trans influence of R, and (c) the C−M−P angle increases due to steric repulsions between PH_3 and R ligands (Tables S3 and S4). Thus, the energetics of the breaking M−R bond during the C−C coupling process depends on the directionality of ligand orbitals and the steric repulsion between R and L ligands.

On the basis of the discussion presented above, we rationalize the calculated trends in thermodynamic and kinetic properties of the reductive elimination reactions studied as follows. When the ΔH values (exothermicity) are similar (**1**−**3**), the kinetics of the C−C bond formation is determined by the orientation (including directionality of the M−C bond and steric interaction between R and L ligands) effect, which decreases in the order Me−Me > Ph−Ph > Vin−Vin. Among the reactions with large difference in ΔH (**1**−**3** vs **4**) the activation barrier is strongly influenced by the exothermicity of the reaction according to the Hammond postulate. A combination of these two factors explains the calculated trend in the ease of the C−C bond formation reaction in the $R_2M(PH_3)_2$ complexes: Vin−Vin > Ph−Ph > Eth−Eth > Me−Me.

C. Reductive Elimination from Asymmetrical $RR'M(PH_3)_2$ Complexes (M = Pd, Pt). As expected, the asymmetrical C−C coupling (R, R′ = Me, Vin, Eth, Ph; R ≠ R′) also proceeds through a three-centered transition state similar to the symmetrical one discussed above (Figures 1 and S2). The results presented in Table 3 clearly show that the calculated barriers and reaction energies for asymmetrical R−R′ coupling in $RR'M(PH_3)_2$ complexes are close to an average between the corresponding barriers of the symmetrical R−R and R′−R′ coupling reactions in $R_2M(PH_3)_2$ and $R'_2M(PH_3)_2$, respectively.

$$\Delta H(\mathrm{R-R'}) \approx (\Delta H(\mathrm{R-R}) + \Delta H(\mathrm{R'\text{-}R'}))/2$$

$$\Delta H^{\ddagger}(\mathrm{R-R'}) \approx (\Delta H^{\ddagger}(\mathrm{R-R}) + \Delta H^{\ddagger}(\mathrm{R'\text{-}R'}))/2$$

As seen in Table 4, the predicted values of ΔH(R−R′) and $\Delta H^{\ddagger}$(R−R′) using these equations are only 1 and 2 kcal/mol different from their calculated values, respec-

(31) During the constrained optimization the value of α was frozen and the square-planar geometry of the metal complex was maintained. All the other geometry parameters were optimized.

(32) For a graphical representation, see Scheme 2 and Figure S4.

Table 4. Calculated[a] and Predicted[b] Activation ($\Delta H^{\ddagger}$) and Reaction (ΔH) Enthalpies of the Reaction $RR'M(PH_3)_2 \rightarrow R\text{-}R' + M(PH_3)_2$ for the Asymmetrical Complexes (in kcal/mol)[c]

		$\Delta H^{\ddagger}$		ΔH	
no.	complex	calcd	predicted	calcd	predicted
5	$M(CH_3)(CH{=}CH_2)(PH_3)_2$	15.5 (32.2)	15.1 (31.5)	−29.4 (−14.5)	−31.8 (−16.5)
6	$M(CH_3)(Ph)(PH_3)_2$	17.5 (36.4)	17.4 (35.7)	−30.0 (−14.6)	−30.8 (−15.5)
7	$M(CH_3)(C{\equiv}CH)(PH_3)_2$	20.6 (38.3)	18.6 (36.2)	−20.7 (−5.7)	−24.3 (−8.1)
8	$M(CH{=}CH_2)(Ph)(PH_3)_2$	8.6 (23.1)	8.2 (22.3)	−31.4 (−15.7)	−32.2 (−16.6)
9	$M(CH{=}CH_2)(C{\equiv}CH)(PH_3)_2$	10.2 (24.3)	9.5 (22.9)	−22.8 (−6.7)	−25.7 (−9.2)
10	$M(Ph)(C{\equiv}CH)(PH_3)_2$	10.8 (25.4)	11.8 (27.1)	−23.6 (−7.6)	−24.6 (−8.2)

[a] The values were taken from Table 3. [b] The predicted values are average of those symmetric complexes taken from Table 3. [c] Values for M = Pd are given without parentheses, while those for M = Pt are given in parentheses.

tively. These discussions clearly indicate the additive nature of the calculated energetics of C−C coupling reactions.

Most likely, the relationships deduced above are valid for other asymmetrical coupling reactions involving substituted alkyl, vinyl, phenyl, and ethynyl groups, as well as different transition-metal complexes. This conclusion provides a simple tool to predict the C−C coupling barriers and reaction energies of asymmetrical coupling reactions from symmetrical coupling reactions.[33] One might expect that the predicted simple relationships will provide important information for rationalizing existing experimental observations, predicting byproduct formation, and more. However, one should note that the relationships provided above are only valid in the case of a negligible interaction (steric and electronic) existing between the organic ligands (R, R′) in the transition-metal complex. Obviously, the complexes studied in the present work meet this criterion.

D. Difference Between Palladium and Platinum Complexes in the C−C Coupling Reactions. In all the cases studied, reductive elimination involving Pd complexes requires smaller activation barriers, by 12−21 kcal/mol, and is more exothermic by a similar amount, 14−16 kcal/mol, compared to the corresponding Pt complexes (Table 3). Clearly, C−C coupling reactions involving Pd complexes will proceed much more easily than the same process with Pt complexes. This conclusion is in excellent agreement with available experiments, where more active Pd complexes are utilized in the catalytic coupling reactions, while Pt complexes are more stable and were isolated.[1−12] The present study confirms the general trend of relative reactivity order Pd > Pt for a broad class of C−C coupling reactions.

The presented difference in the barrier heights and energies of reaction between Pd and Pt complexes is clearly related to the destabilization of the initial Pd complex, relative to the transition state and products, by roughly 16 kcal/mol, compared to the Pt complexes. This in turn relates to the M−R(R′) bond strength in these complexes, which was shown (see Table 2) to be roughly 8 kcal/mol stronger for M = Pt than for M = Pd.

E. Comparison with Available Experimental Results. Experimentally it was generally established that reductive elimination of two methyl ligands is much more difficult compared to the same process involving unsaturated groups[1−5] and that the high activation barrier of the C−C reductive elimination reactions imposes several limitations to the practical utilization of catalytic alkyl−alkyl coupling.[1] Meanwhile, the high reactivity of the unsaturated ligands very often is the reason for an inability to observe the PdRR′ (where R and R′ are not Me) intermediates,[1,3] which could be isolated only by introducing at least one methyl ligand.[1,3,34] These observations agree very well with the computational findings of the present paper.

For the coupling reactions involving phenyl ligands the following reactivity order has been established for palladium complexes: diaryl > aryl alkyl > dialkyl.[2a] Our calculations are in excellent agreement with this experimental finding.

It is worth mentioning that in an elegant study of C−C coupling on Ir^{III} complexes Maitlis and co-workers have shown the following reactivity order in the carbon−carbon bond formation reaction: Vin−Vin > Vin−Me > Ph−Me > Me−Me,[35] which is in excellent agreement with our results for palladium and platinum complexes, suggesting a similar nature of the C−C coupling reaction for other transition-metal complexes.[36]

A comparative study of the unsaturated ligands has indicated the higher reactivity of the alkenyl group over aryl, alkynyl, or alkyl groups in reductive elimination reactions from palladium complexes.[34] The higher reactivity of the alkenyl group is in line with our computational study.

Finally, the experimentally measured activation energy of 21 kcal/mol for the alkenyl−alkynyl coupling on a platinum complex[24] is in reasonable agreement with our model calculations: $\Delta H^{\ddagger}$ = 24.3 kcal/mol (entry 9, Table 3).

Despite the reliability of the computational approaches adopted and a wide range of reactions studied, the limits of the present work should be clearly stated. The calculated relative reactivity in the C−C coupling reaction may not be directly compared to the overall reactivity in the catalytic cycle. In addition to the C−C reductive elimination, the catalytic C−C cross-coupling reactions include the oxidative addition and transmetalation steps[1−12] and have to be taken into account as well. Instead, the present study should assist in identifying the rate-determining step of the C−C coupling catalytic cycles, which in fact is one of the most difficult problems in this area.[1−12] Care should be taken to compare the present results obtained for reductive elimination reactions from the *cis*-$[M(R)(R')(PH_3)_2]$ complexes with multistep C−C coupling reactions involving

(33) With modern computational software the C_2 point group for such metal complexes reduces the computational cost by about 1.5−2 times.

(34) Negishi, E.; Takahashi, T.; Akiyoshi, K. *J. Organomet. Chem.* **1987**, *334*, 181.
(35) Maitlis, P. M.; Long, H. C.; Quyoum, R.; Turner, M. L.; Wang, Z.-Q. *Chem. Commun.* **1996**, 1.
(36) In the case of cobalt(III) complexes it was also shown that Vin−alkyl reductive elimination is more favorable than alkyl−alkyl; see: Evitt, E. R.; Bergman, R. G. *J. Am. Chem. Soc.* **1980**, *102*, 7003.

cis/trans isomerization or ligand dissociation.[37] Obviously, in any multistep process, either catalytic or noncatalytic, the overall reactivity may depend on other factors as well.

5. Conclusions

From the findings and discussions presented above, we can draw the following conclusions.

(i) The C−C cross-coupling barrier from the symmetrical $R_2M(PH_3)_2$ (where M = Pd, Pt) complex decreases in the order R = Me > Eth > Ph > Vin: i.e., the Me−Me coupling is the most energy demanding, while the Vin−Vin coupling is the least demanding among the complexes studied. All reductive elimination reactions studied are exothermic, and their exothermicity changes in the following order Vin−Vin ≈ Ph−Ph ≈ Me−Me > Eth−Eth.

(ii) For reactions with similar exothermicity (ΔH) values, the kinetics of the C−C bond formation is mainly determined by the orientation (including directionality of the M−C bond and steric interaction between the R and L ligands) effect. For the reactions with a large difference in exothermicity, the activation barrier is strongly influenced by the thermodynamics, in agreement with the Hammond postulate. The combination of these two factors explains the overall trend in the ease of C−C bond formation in the $R_2M(PH_3)_2$ complexes: Vin−Vin > Ph−Ph > Eth−Eth > Me−Me.

(iii) The barriers, $\Delta H^{\ddagger}$(R−R′), and the exothermicities of reaction, ΔH(R−R′), for asymmetrical R−R′ coupling in $RR'M(PH_3)_2$ are very close to the averages of the corresponding values of the symmetrical R−R and R′-R′ coupling reactions in $R_2M(PH_3)_2$ and $R'_2M(PH_3)_2$:

$$\Delta H(\text{R}-\text{R}') \approx \Delta H(\text{R}-\text{R})/2 + \Delta H(\text{R}'-\text{R}')/2$$

$$\Delta H^{\ddagger}(\text{R}-\text{R}') \approx \Delta H^{\ddagger}(\text{R}-\text{R})/2 + \Delta H^{\ddagger}(\text{R}'-\text{R}')/2$$

We believe that these simple rules should be valid for other asymmetrical coupling reactions involving substituted alkyl, vinyl, phenyl, ethynyl, or other organic ligands as well as for different transition-metal complexes. This provides a simple tool to predict C−C coupling barriers and reaction energies of asymmetrical coupling reactions, both qualitatively and quantitatively with reasonable precision, having calculated only symmetrical coupling reactions.

(iv) The C−C coupling reactions involving methyl, vinyl, phenyl, and ethynyl ligands occur much easier in Pd than in Pt complexes, because the Pd−R(R′) bond energy is smaller that the Pt−R(R′) bond energy. Generalizing this finding, we can predict that, the weaker the M−R(R′) bond, the easier the C−C cross-coupling reaction.

At the end let us note that, although the absolute values of C−C coupling barriers and reaction energies may depend on the method and basis set used and also may be influenced by substitution effects in R and phosphine ligands, we believe that the relative reactivity order and major conclusions of the present study will remain valid for a broad class of C−C coupling reactions. To the best of our knowledge, this work is the first detailed theoretical study of carbon−carbon bond formation through the reductive elimination process involving unsaturated organic ligands.

Acknowledgment. V.P.A. acknowledges the Visiting Fellowship at the Cherry L. Emerson Center of Emory University. The present research has been supported in part by a grant (No. CHE-0209660) from the National Science Foundation. Acknowledgment is also made to the Cherry L. Emerson Center of Emory University for the use of its resources.

Supporting Information Available: Carbon−carbon bond dissociation energy of organic products R−R′ (Table S1), tilt angle dependence of the Pt−C distance in the vinyl complex $[Pt(CH{=}CH_2)_2(PH_3)_2]$ (Table S2), calculated relative energy and some geometry parameters for the model complexes $[Pd^{II}(R)(PH_3)_3]^+$ as a function of α angle (Table S3), calculated relative energy and some geometry parameters for the model complexes $[Pt^{II}(R)(PH_3)_3]^+$ as a function of α angle (Table S4), Cartesian coordinates of all calculated structures in this paper (Table S5), schematic presentation of the symmetrical R−R coupling reactions from the $RRM(PH_3)_2$ complexes studied in this paper (Figure S1), schematic presentation of the asymmetrical R−R′ coupling reactions from the complexes $RR'M(PH_3)_2$ (Figure S2), top views of the representative points of tilt angle dependence on the value of Pt−C distance (Figure S3), calculated important bond distances (in Å) of products of the C−C coupling from the complexes $RR'M(PH_3)_2$ studied in this paper (Figure S4), graphical representation of the α angle for the model $[M(R)(PH_3)_3]^+$ complexes studied in this paper (Figure S5), and optimized geometry structures of some platinum π-complexes and dissociation transition state (Figure S6). This material is available free of charge via the Internet at http://pubs.acs.org.

OM0490841

(37) For a general discussion of possible reductive elimination mechanisms see: Collman, J. P.; Hegedus, L. S.; Norton, J. R.; Finke, R. G. *Principles and Application of Organotransition Metal Chemistry*; University Science Books: Mill Valley, CA, 1987.